Temperature Dependence of the Electron–O_2^+-Ion Recombination Coefficient*

W. H. Kasner and Manfred A. Biondi†
Westinghouse Research Laboratories, Pittsburgh, Pennsylvania 15235
(Received 7 May 1968)

The temperature dependence of the coefficient for the recombination of electrons with mass-identified O_2^+ ions has been determined from observations of the electron and ion decay rates in the afterglow following "single-pulse" microwave discharges in O_2-Ne, O_2-Ne-Ar, and O_2-Ne-Kr gas mixtures. Temporal mass analysis, utilizing multichannel signal-averaging techniques, shows similar decay rates for the electrons and for the O_2^+ ions over the major portion of the afterglow. The observed recombination coefficient, $\alpha(O_2^+)$, has a temperature dependence approximated by T_{gas}^{-1}, the values at temperatures of 205, 295, and 690°K being $(3.0 \pm 0.3)\times10^{-7}$, $(2.2 \pm 0.2)\times10^{-7}$, and $(1.0 \pm 0.2)\times10^{-7}$ cm^3/sec, respectively. At the lower temperatures the dimer ion $O_2 \cdot O_2^+$ becomes significantly more important. Analysis of the data yields a coefficient of approximately 2.3×10^{-6} cm^3/sec for the recombination of this ion with electrons at a temperature of 205°K.

I. INTRODUCTION

One of the principal ionospheric positive ions in the altitude range 75 – ~200 km has been shown[1] to be O_2^+. Analyses[2] of the relevant atomic collision reactions indicate that the rate of removal of electrons from this region is to a large extent controlled by dissociative recombination of the electrons with O_2^+ ions. Therefore, as a continuation of our program of laboratory measurements of atomic collision rates of ionospheric interest, we have undertaken extensive afterglow studies of the recombination coefficient for electrons with O_2^+ ions over the temperature range 205 – 690°K. These studies are somewhat more difficult than the related N_2^+ measurements,[3,4] in that problems arise in producing a plasma with O_2^+ ions in their ground electronic state and in avoiding negative-ion accumulation, with attendant effects on the afterglow decay.

In the following sections we describe the modifications of the afterglow-measuring technique required for the oxygen studies and discuss the atomic collision processes leading to production of O_2^+ ions in their ground electronic state. We then analyze the measurements to obtain the temperature dependence of the coefficient $\alpha(O_2^+)$ for the recombination of electrons and O_2^+ ions, and to obtain an approximate value of the coefficient $\alpha(O_4^+)$ for the recombination of electrons and O_4^+ ions at 205°K.

II. EXPERIMENTAL METHOD

The apparatus combines the microwave technique for determining average electron densities during the afterglow with a differentially pumped mass spectrometer which samples the ions diffusing to the wall of the microwave cavity. Inasmuch as most of the apparatus has been described in detail in previous papers,[3,4] we shall elaborate on only those additional features required for the oxygen study.

The microwave cavity and mass spectrometer are shown schematically in Fig. 1. In the operation of the microwave system (see Fig. 1 of Ref. 3), a pulse from a magnetron (~2-msec duration) is used to ionize the gas in the cavity. A low-energy probing microwave signal is used to determine the resonant frequency of the cavity at successive times during the afterglow, from which the average electron density at each of these times can be calculated.

In order to avoid negative-ion accumulation from one discharge-afterglow cycle to the next, the apparatus is operated in a "single-pulse–afterglow" mode in which the plasma is permitted to decay for approximately 10 sec between cycles. Reproducible plasma generation from cycle to cycle is assured by providing initiating electrons from an electrode (see Fig. 1) to which is applied a 1 kV, 50 μsec impulse at the beginning of each discharge.

The differentially-pumped mass spectrometer shown in Fig. 1 samples ions diffusing to the cavity wall and effusing through a small orifice, as in the earlier studies of nitrogen.[3,4] With the single-pulse–afterglow technique, the signals

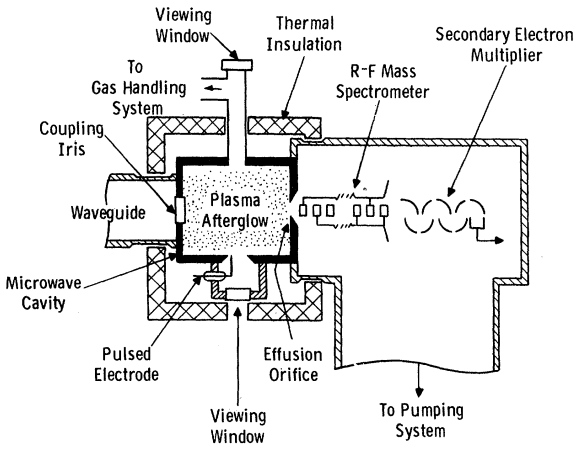

FIG. 1. Schematic view of the microwave afterglow apparatus showing the microwave cavity and the radio-frequency mass spectrometer.

are correspondingly smaller than in the nitrogen work, where the discharge-afterglow cycle was repeated some 40 times per second. We have, therefore, employed a signal accumulation technique to obtain accurate measurements of the ion decay during the afterglow. To this end, the afterglow is divided into 100 equal time intervals of 300–600 μsec duration. The voltage pulses resulting from the transit of single ions through the mass spectrometer/secondary electron multiplier (see Fig. 1) are fed through an amplifier and discriminator into a T.M.C. Model 400C "CAT" operating in a multiscaling mode. As the "CAT" advances from channel to channel, the numbers of ions counted in the corresponding time intervals in the afterglow are recorded in the memory section. By accumulating the afterglow counts for 100–1000 single-pulse–afterglow cycles, statistical fluctuations in the data are reduced to low levels (<10%).

III. RELEVANT AFTERGLOW PROCESSES

In order to simplify the analysis of the afterglow sufficiently to yield quantitative determinations of the recombination coefficient $\alpha(O_2^+)$, it is necessary to achieve conditions in which O_2^+ is the only significant afterglow ion and electron-ion recombination dominates the volume loss of electrons. The formation of complex ions, e.g., O_3^+ and O_4^+, is reduced by use of small concentrations of O_2 molecules [$p(O_2) \sim 10^{-3}$ Torr], and the addition of an "inert" neon buffer gas [$p(Ne) \sim 20$ Torr] inhibits diffusion to the walls. In such a mixture, one of the dominant production mechanisms for O_2^+ is the Penning reaction

$$Ne^M + O_2 \rightarrow Ne + O_2^+ + e, \qquad (1)$$

where the superscript M indicates a metastable excited state. Unfortunately, in this reaction there is sufficient excitation energy to create the ions not only in the desired ground electronic state ($X^2\Pi_g$) but also in the excited electronic state ($a^4\Pi_u$). For this reason, we have used triple mixtures, adding approximately 1 Torr of Ar, or Kr, to the O_2-Ne mixtures in an attempt to produce O_2^+ ions in only the $X^2\Pi_g$ state. Assuming comparable cross sections for the Penning ionization of O_2 and Ar (or Kr)[5] by neon metastable atoms and using the relevant charge-transfer cross sections,[6] it appears that the probable ion production sequence in the triple gas mixtures involves Penning ionization of Ar (or Kr) by the neon metastable atoms, followed by charge transfer of the resulting Ar^+ (or Kr^+) ions with O_2 to form O_2^+.[7] In the Kr^+ charge-transfer reaction, the available energy is not sufficient to excite the O_2^+ ions beyond the $v = 8$ vibrational level of the *ground* electronic state.

A second reason for using as small a neutral O_2 density as practicable is to avoid appreciable negative-ion formation during either the discharge or the afterglow. It has been shown[8,9] that the electron ambipolar-diffusion loss rate increases in proportion to the negative-ion/electron-concentration ratio. In addition, positive-ion–negative-ion recombination must be considered if this ratio is not small compared with unity. Use of the single-pulse–afterglow technique mentioned earlier is dictated by the fact that, even if the negative-ion production by electron attachment is small in a given discharge-afterglow cycle, the negative ions are essentially trapped in the plasma[8,9] and their concentration will build up unless sufficient time elapses between cycles to permit the plasma to decay completely.

Having chosen conditions in which O_2^+ in the desired state is the only significant positive ion (negative ions being essentially absent) and electron-ion recombination is the principal electron loss process, we may approximate the electron continuity equation during the afterglow by

$$\partial n_e/\partial t = -\alpha n_e^2 + D_a \nabla^2 n_e , \qquad (2)$$

where α and D_a are recombination and ambipolar-diffusion coefficients, respectively. We have invoked the quasineutrality of a plasma to set $n_+ \approx n_e$. In spite of the fact that volume recombination greatly outweighs ambipolar diffusion in determining the electron loss rate, the diffusion term has been included, inasmuch as it has a pronounced effect on the spatial distribution of the electrons within the microwave cavity.

Computer solutions of Eq. (2), subject to the boundary condition $n_+ = n_e \approx 0$ at the walls of the cavity,[10,11] permit us to obtain quantitative determinations of α from the measured rates of decay of the average electron density during the afterglow. The particular average used in the present analysis, the so-called "microwave-average" electron density, is defined by

$$\bar{n}_{\mu w}(t) \equiv \frac{\int_V n_e(\vec{r}, t) E^2(\vec{r}) dV}{\int_V E^2(\vec{r}) dV} = \Delta f(t)/C , \qquad (3)$$

where $E(\vec{r})$ is the electric field of the microwave probing signal. The integration extends over the volume of the cavity. This average has the virtue that its value does not depend upon assumptions concerning the form of the electron distribution within the cavity; it is simply equal to the measured cavity frequency shift $\Delta f(t)$, divided by a group of physical constants C.[12] In addition, in the present case where the plasma fills the entire cavity volume, $\bar{n}_{\mu w}(t)$ has the same value as the electron density obtained from $\Delta f(t)$ on the artificial assumption that the electrons are uniformly distributed throughout the volume. (This assumption has been widely used previously.[13])

The elementary "recombination solution" of Eq. (2) which results when the diffusion term is neglected is

$$1/\bar{n}_{\mu w}(t) = 1/\bar{n}_{\mu w}(0) + at, \qquad (4)$$

where the slope of the curve a is related to the desired recombination coefficient α. In many cases it is convenient to plot our data as the reciprocal of $\bar{n}_{\mu w}(t)$ versus afterglow time to display recom-

bination control of the afterglow. Recombination coefficients α may be obtained from the slopes a of the straight-line sections in these $1/\bar{n}_{\mu w}(t)$-versus-time curves by using appropriate correction factors.[10,11] Alternatively, we can obtain α by making a direct comparison of the measured $\bar{n}_{\mu w}(t)$ with the predicted $\bar{n}_{\mu w}(t)$ curves obtained by computer solution of Eq. (2) when known values of D_a are inserted and α is treated as a parameter.[11,14]

IV. RESULTS AND DISCUSSION

To ensure quantitative measurements of the rate of recombination of O_2^+ ions with electrons, two key requirements should be met. First, the average electron density decay should follow the form given by the computer solution of Eq. (2) for recombination-controlled conditions. This, in turn, implies that a linear increase of $1/\bar{n}_{\mu w}(t)$ with time [see Eq. (4)] be observed for an appreciable electron density range. Secondly, O_2^+ should be the only significant afterglow ion, and its observed wall current (the mass-spectrometer output) should approximately follow the volume electron density decay during the afterglow. The first condition has been achieved by assuring that no significant ionization occurs during the afterglow and that the ambipolar diffusion rate is small. A simple optical absorption system[3] making use of an optical path through the plasma via the viewing windows (See Fig. 1) monitors the neon metastable concentration. Thus we are able to choose a discharge pulse length which leads to a small enough metastable density at the start of the afterglow[3] that the rate of Penning ionization, reaction (1), is negligible. As noted earlier, the ambipolar diffusion to the walls is made very small by use of a high (~20 Torr) pressure of neon buffer gas.

The expectation that the O_2^+ wall current should approximately follow the volume electron density decay arises from the fact that the computer solution of the positive-ion continuity equation [which is identical to Eq. (2) with n_+ replacing n_e everywhere] indicates that for much of the afterglow the *form* of the ion and electron density distributions within the cavity remains approximately constant (cf. Gray and Kerr[10]). Thus the ion diffusion current to the wall, which is proportional to $(\nabla n_+)_{\text{wall}}$, decreases approximately as n_+ (and hence n_e) decreases in the volume.

An example of the observed electron and ion decays is shown in Fig. 2 for a binary mixture of oxygen (1.1×10^{-3} Torr) and neon (20 Torr) at 295°K. It will be seen that $1/\bar{n}_{\mu w}(t)$ increases linearly with time over a density range, $f\approx10$, and that after approximately 4 msec the reciprocal of the O_2^+ wall current follows the electron decay (O_2^+ is the only significant afterglow ion). The solid line represents the predicted electron density decay obtained from the computer solution[14] of Eq. (2) with $D_a p = 360$ (cm²/sec) Torr for O_2^+ ions in neon[15] and a value of $\alpha(O_2^+) = 2.2\times10^{-7}$ cm³/sec. This computation uses an initial electron and ion distribution which is a fundamental-mode diffusion distribution, reasonably approximating the actual starting distribution created by the microwave discharge. In addition, after $\lesssim$1 msec the predicted decays are rather insensitive to the starting distribution[11,16] unless extreme forms, such as highly constricted plasmas, are used.

It is interesting to note that if the measured slope of Fig. 2 is corrected using the Gray and Kerr correction factors[10] corresponding to a spherical plasma container having a fundamental diffusion length, $\Lambda = 1.125$ cm, equal to that of our rectangular parallelepiped cavity, a value $\alpha(O_2^+) = 2.1\times10^{-7}$ cm³/sec is obtained. This result is in good agreement with the value obtained by computer solution for the rectangular geometry. Therefore, for most of the experimental data, we have obtained corrected values of the recombination coefficient by applying Gray and Kerr correction factors in the above manner, rather than by obtaining computer solutions for each decay curve.

In the early phases of this study, binary O_2-Ne mixtures were used for the recombination measurements. When "single-pulse-afterglow" techniques were employed, linear $1/\bar{n}_{\mu w}(t)$ versus time curves were obtained with satisfactory tracking of the electron density and O_2^+ wall-current decays. However, unlike the recombination studies in nitrogen[3,4] where the values of $\alpha(N_2^+)$ did not depend

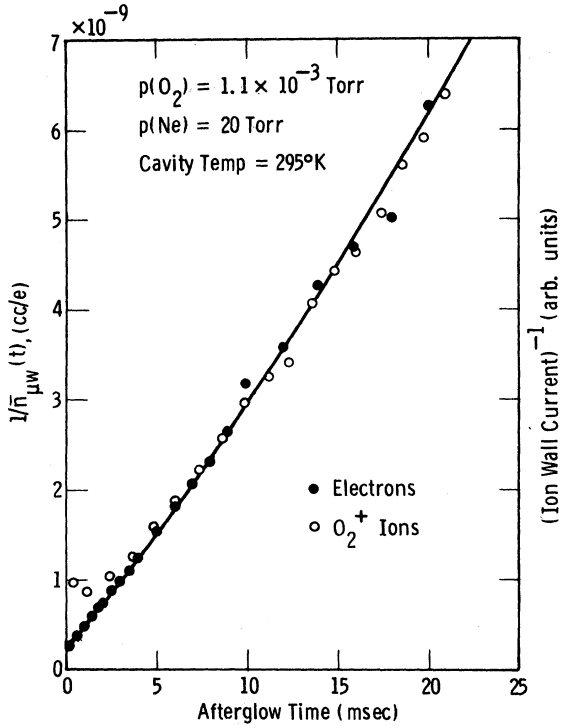

FIG. 2. Reciprocal plots of observed electron density and O_2^+ wall currents as functions of time in the afterglow of an O_2-Ne microwave discharge. The O_2^+ wall currents have been normalized to the electron density at an afterglow time of 6 msec. The solid line represents a numerically computed fit of the electron continuity equation to the observed electron density, taking into account both the recombination and ambipolar-diffusion loss mechanisms.

on the N_2 partial pressure, the coefficient $\alpha(O_2^+)$ varied significantly with the partial pressure of O_2 used, as is shown by the short-dashed curve of Fig. 3.

A possible explanation of the observed variation in $\alpha(O_2^+)$ with O_2 pressure in the binary mixtures lies in the fact, noted in Sec. III, that more than one electronic state of O_2^+ can be formed in the Penning reaction. In an effort to avoid formation of electronically excited O_2^+ ions, we first added approximately 1 Torr of Ar, then of Kr, to the binary gas mixture. Under these conditions one hopes to excite the $X^2\Pi_g$ state of O_2^+ by the sequence $Ne^M \rightarrow Ar^+$ (or Kr^+) $\rightarrow O_2^+$. Unfortunately, when Ar is added to the binary mixture, the energetics of the charge-transfer reaction from Ar^+ still permit excitation of many ($v > 20$) vibrational levels of the $X^2\Pi_g$ state of O_2^+, and, as indicated by the long-dashed line in Fig. 3, also yields a significant variation of $\alpha(O_2^+)$ with changing oxygen pressure. When Kr is added to the O_2-Ne mixture, a much weaker dependence of $\alpha(O_2^+)$ on oxygen pressure is noted (solid curve of Fig. 3). Here, only the lower vibrational levels ($v \leq 8$) of the O_2^+ ground electronic state can be excited in the charge transfer from Kr^+. In the discussion of the temperature-dependence measurements which follow, we have included data obtained in O_2-Ne and O_2-Ne-Kr mixtures. The observed recombination coefficients obtained using O_2-Ne-Kr mixtures show no significant dependence on the oxygen pressure except at the lowest temperature investigated (205°K). The O_2 densities (3.5×10^{13}–2.5×10^{14} cm^{-3}) used in obtaining experimental data in O_2-Ne mixtures correspond to the O_2 pressure range (1×10^{-3} to 8×10^{-3} Torr) in Fig. 3 over

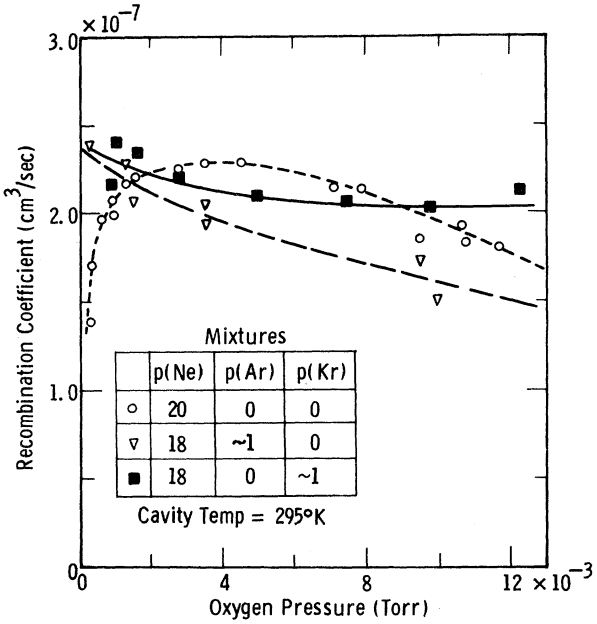

FIG. 3. Observed oxygen pressure dependence of the recombination coefficient $\alpha(O_2^+)$. The short-dashed, long-dashed, and solid lines correspond to O_2-Ne, O_2-Ne-Ar, and O_2-Ne-Kr gas mixtures, respectively.

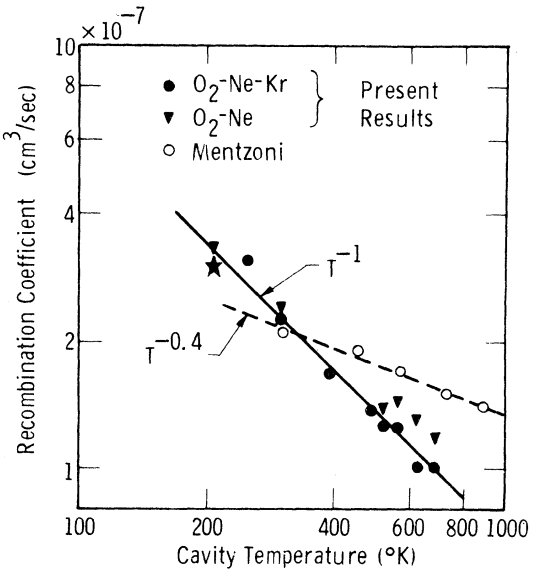

FIG. 4. Log-log plot of the observed temperature dependence of the coefficient for the recombination of O_2^+ ions and electrons obtained from afterglow studies in O_2-Ne and O_2-Ne-Kr gas mixtures. The single point (★) is an estimated value of $\alpha(O_2^+)$ obtained under conditions where O_4^+ was a significant afterglow ion (see text and Fig. 5).

which $\alpha(O_2^+)$ shows the least variation. In no case have we observed a significant dependence of $\alpha(O_2^+)$ on the pressure of the neon buffer gas.

In order to obtain values of $\alpha(O_2^+)$ at temperatures above and below 295°K, the cavity has been thermally isolated from the rest of the apparatus[4] and either a heater or a refrigerating bath placed inside of the thermal insulation shown in Fig. 1. At temperatures above approximately 500°K, significant concentrations of impurity ions, presumably resulting from thermal desorption from the cavity walls, are observed in the mass spectra. By means of an auxiliary pumping line attached to the cavity (not shown in Fig. 1) it has been possible to significantly increase the gas flow rate and effectively reduce the impurity concentration, thereby permitting operation at higher temperatures. In this way afterglow measurements have been obtained over the temperature range 205–690°K.

The results of the measurements of the temperature dependence of $\alpha(O_2^+)$ are shown by the solid data points in the log-log plot of Fig. 4; the triangular points indicate the O_2-Ne mixture results, while the solid circles indicate the O_2-Ne-Kr mixture results. In nearly all cases these data points represent the average of several measurements of $\alpha(O_2^+)$ at the respective temperatures. The single point (★), corresponding to a temperature of 205°K, is a derived value for $\alpha(O_2^+)$ obtained under conditions where O_4^+ was a significant afterglow ion. The method of obtaining $\alpha(O_2^+)$ in this case will be discussed in more detail shortly. In most of the experimental data presented in Fig. 4, we observed similar decay rates for the electron den-

sity and the O_2^+ wall currents. The exceptions occurred at 205°K, where significant O_4^+ concentrations were observed, and at the highest temperature, ~690°K, where the O_2^+ wall current decayed at a somewhat slower rate than $\bar{n}_{\mu W}$. At present we have no explanation for the observed difference in the decay rates at the higher temperatures.

For purposes of comparison, we have also included in Fig. 4 the results obtained by Mentzoni[17] for unidentified ions in oxygen. One notes that at room temperature (~295°K) the present results are in good agreement with those of Mentzoni. However, our observed temperature dependence, which is reasonably well represented by the relation $\alpha(O_2^+) \propto T^{-1}$ (the solid line), is significantly stronger than that indicated by Mentzoni's data (the dashed line).

It has been noted that the measured recombination coefficients obtained at low temperatures (205°K) from O_2-Ne-Kr mixtures exhibit a significant dependence on the oxygen pressure. In addition, the observed recombination coefficients seem unusually large, the values ranging from 8.0×10^{-7} to 2.5×10^{-6} cm³/sec. The corresponding value of $\alpha(O_2^+)$ obtained from O_2-Ne mixtures is 3.3×10^{-7} cm³/sec (see Fig. 4). Mass-spectrometer studies indicate that the abnormal behavior observed in O_2-Ne-Kr mixtures at the low temperatures is related to the appearance of O_4^+ as a significant afterglow ion. In this case the observed decay rates of the O_4^+ and O_2^+ ions are quite similar, suggesting an essentially constant $[O_4^+]/[O_2^+]$ concentration ratio during the afterglow, and hence a thermodynamic equilibrium behavior.

If such an equilibrium behavior does exist, it is a simple matter to show that the electron density decay will follow the form of Eq. (4) with the slope yielding an effective recombination coefficient, α_{eff}, given by

$$\alpha_{\text{eff}} = (R_0\alpha_4 + \alpha_2)/(R_0 + 1), \tag{5}$$

where $\alpha_4 = \alpha(O_4^+)$, $\alpha_2 = \alpha(O_2^+)$, and R_0 is the equilibrium ratio of the $[O_4^+]/[O_2^+]$ ion densities within the cavity. From this expression we note that a plot of $\alpha_{\text{eff}}(R_0+1)$ versus R_0 should yield a straight line having a slope α_4 and an intercept α_2. This predicted behavior is not followed if we assume that the *measured* ion current ratio R is an accurate representation of the equilibrium ion density ratio R_0. In the present experiment it is quite possible that discrimination against the weakly bound O_4^+ ions takes place in drawing the ions from the microwave cavity as a result of breakup collisions in the ion accelerating region, in which case, $R_0 > R$. Using our measured oxygen pressure data and extrapolating the O_4^+-O_2^+ equilibrium constant obtained by Yang and Conway[18] to our temperature (205°K) we find that the computed $[O_4^+]/[O_2^+]$ density ratio in the cavity is approximately 5.5 times larger than the corresponding measured O_4^+/O_2^+ ion wall-current ratio. The data presented in Fig. 5 are based on this relation, $R_0 = 5.5R$. In this case a straight line dependence on R_0 is obtained, the slope and intercept of the line yielding recombination coefficients $\alpha(O_4^+) \cong 2.3 \times 10^{-6}$ cm³/sec and $\alpha(O_2^+) \cong 3 \times 10^{-7}$ cm³/sec, respectively.[19]

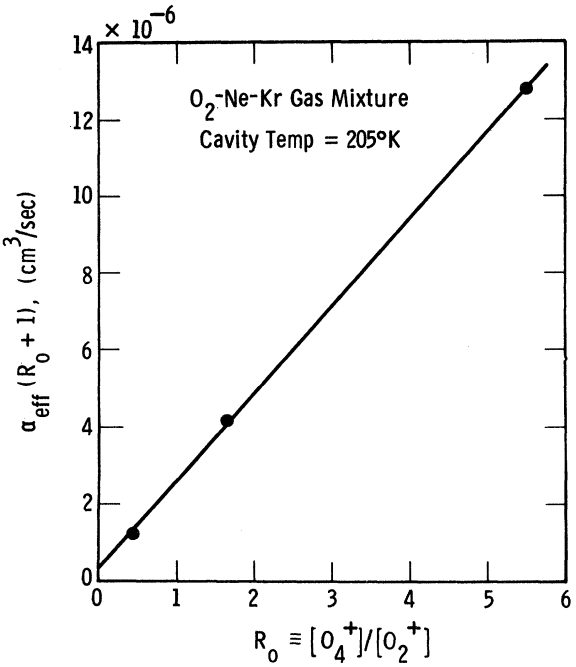

FIG. 5. Dependence of the effective recombination coefficient α_{eff} on the $[O_4^+]/[O_2^+]$ concentration ratio R_0. α_{eff} has been multiplied by the factor (R_0+1) in order to show the fit of the experimental data to Eq. (5). The slope and intercept of the solid line yield recombination coefficients $\alpha(O_4^+) \cong 2.3 \times 10^{-6}$ cm³/sec and $\alpha(O_2^+) \cong 3 \times 10^{-7}$ cm³/sec, respectively.

Thus it appears that the anomalous behavior at low temperatures can indeed be explained by the fact that the weakly bound O_4^+ ions, which have a large recombination coefficient, become increasingly important at low temperatures.

V. CONCLUSIONS

From the foregoing discussion we conclude that the values of $\alpha(O_2^+)$ for O_2^+ ions in the $X^2\Pi_g$ ground electronic state vary from $(3.0 \pm 0.3) \times 10^{-7}$ cm³/sec at $T_e = T_+ = T_{\text{gas}} = 205$°K to $(1.0 \pm 0.2) \times 10^{-7}$ cm³/sec at 690°K (see Fig. 4). As a result of the mode of ion formation, it is energetically possible that the O_2^+ ions are created in an excited vibrational state ($v \leq 8$). However, inasmuch as the recombination loss is studied over some 10 msec of the afterglow, there may be time for the initial vibrational excitation to decay to the $v = 1$ state via vibration exchange collisions[20] with O_2 molecules of the type $(v, O) \rightarrow (v - 1, 1)$ before recombination occurs. Thus the present values of $\alpha(O_2^+)$ probably refer to ions in the same state as those which are produced in the ionosphere by photo-ionization and are therefore appropriate for use in ionospheric model calculations.

The analysis of the contribution of O_4^+ ions to the recombination loss at 205°K leads to an approximate value $\alpha(O_4^+) = 2.3 \times 10^{-6}$ cm³/sec. It is interesting

to note that this value is about the same order of magnitude as that obtained[3] for $N_4^+[\alpha(N_4^+) \approx 2\times10^{-6}$ cm^3/sec at 300°K] and for the dimer ion $NO \cdot NO^+$ $[\alpha(NO \cdot NO^+) \approx 1.7\times10^{-6}$ cm^3/sec at 300°K].[21] Thus it appears that the dimer ions, $O_2 \cdot O_2^+$, $N_2 \cdot N_2^+$, and $NO \cdot NO^+$, all exhibit substantially larger recombination coefficients than the corresponding monomer ions.

VI. ACKNOWLEDGMENTS

The authors wish to thank the members of the Atomic and Molecular Sciences Directorate for their interest and helpful suggestions concerning this investigation. The authors are also indebted to Lothar Frommhold for providing computer solutions of the continuity equation for our experimental conditions.

---

*This research has been supported in part by the Air Force Weapons Laboratory, Research and Technology Division, Air Force Systems Command, United States Air Force, Kirtland Air Force Base, New Mexico.

†Physics Department, University of Pittsburgh, Pittsburgh, Pennsylvania 15213.

[1]See, for example, R. S. Narcisi and A. D. Bailey, J. Geophys. Res. 70, 3687 (1965); and R. C. Whitten and I. G. Poppoff, Physics of the Lower Ionosphere (Prentice-Hall, Inc., Englewood Cliffs, N. J.).

[2]See, for example, T. M. Donahue, Planetary Space Sci. 14, 33 (1965); E. E. Ferguson *et al.*, J. Geophys. Res. 70, 4323 (1965); and E. E. Ferguson, Rev. Geophys. 5, 305 (1967).

[3]W. H. Kasner and M. A. Biondi, Phys. Rev. 137, A317 (1965).

[4]W. H. Kasner, Phys. Rev. 164, 194 (1967).

[5]Optical absorption measurements in O_2-Ne gas mixtures indicate that the Penning ionization cross section of O_2 by neon metastable atoms is comparable to the value 5×10^{-16} cm^2 obtained for N_2 from similar measurements in N_2-Ne gas mixtures (see Ref. 3). Cross sections for the Penning ionization of Ar by neon metastable atoms have been measured by several observers; e.g., T. G. Schut and J. A. Smit, Physica 10, 440 (1943); M. A. Biondi, Phys. Rev. 88, 660 (1952); and A. V. Phelps and J. P. Molnar, Phys. Rev. 89, 1202 (1953). The measured cross sections range in value from 2.0×10^{-16} to 6.8×10^{-16} cm^2. We have been unable to find any experimental measurements of the Penning ionization cross sections of Kr by neon metastable atoms. However, based on the corresponding measurements for inert gases in helium [see W. P. Jesse and J. Sadauskis, Phys. Rev. 100, 1755 (1955)], we would expect cross section values slightly larger than those obtained for argon in neon.

[6]See, for example, P. D. Golden *et al.*, J. Chem. Phys. 44, 4095 (1966); F. C. Fehsenfeld *et al.*, J. Chem. Phys. 45, 404 (1966).

[7]Some additional confirmation that the direct Penning ionization of oxygen by neon metastable atoms is not a significant O_2^+ production mechanism in the triple mixture comes from the fact that no neon metastable absorption (see Ref. 3) can be detected in the microwave discharges or in the afterglow. Only when the argon, or krypton, is pumped out of the system does the neon metastable atom concentration increase to the point where a detectable absorption signal can be obtained.

[8]M. A. Biondi, Phys. Rev. 109, 2005 (1958).

[9]H. J. Oskam, Philips Res. Rept. 13, 401 (1958).

[10]E. P. Gray and D. E. Kerr, Ann. Phys. (N. Y.) 17, 276 (1962).

[11]L. Frommhold and M. A. Biondi, Plasma Physics Laboratory, University of Texas, Technical Report, 1968 (unpublished); and Ann. Phys. (N. Y.) (to be published).

[12]See, for example, M. A. Biondi, Rev. Sci. Instr. 22, 500 (1951).

[13]See, for example, M. A. Biondi and S. C. Brown, Phys. Rev. 76, 1967 (1949).

[14]L. Frommhold (private communication) has provided computer solutions of Eq. (2) for our experimental conditions.

[15]W. H. Kasner, W. A. Rogers, and M. A. Biondi, Phys. Rev. Letters 7, 321 (1961). See, also, Fig. 6 of L. M. Chanin and M. A. Biondi, Phys. Rev. 107, 1219 (1957).

[16]L. Frommhold, M. A. Biondi, and F. J. Mehr, Phys. Rev. 165, 44 (1968).

[17]M. H. Mentzoni, J. Appl. Phys. 36, 57 (1965).

[18]J. H. Yang and D. C. Conway, J. Chem. Phys. 40, 1729 (1964).

[19]It is interesting to note that if we assume $R_0 = SR$ and then determine the best straight line fit in plots of α_{eff} (R_0+1) versus R_0, using S as a variable parameter, we obtain the result $S=6$, in reasonable agreement with the value determined from the equilibrium constant. The corresponding values of $\alpha(O_4^+)$ and $\alpha(O_2^+)$ are essentially the same as in the text.

[20]Calculations of the vibrational relaxation of O_2^+ ions on O_2 [see, for example, H. Skin, Ion-Molecule Reactions in the Gas Phase, edited by P. J. Ausloos (American Chemical Society Publications, Washington, D. C., 1966), p. 44] indicate that the vibration-to-translation relaxation time for the process $(1,0) \rightarrow (0,0)$ is $\sim$1–10 sec in our experiments. We would expect the vibrational exchange relaxation times for collisions of the type $(v,0) \rightarrow (v-1,1)$ between O_2^+ ions and O_2 molecules to be much shorter, since the vibrational spacing of the ion and molecule are comparable; and hence there is very little transfer of potential energy into kinetic energy.

[21]C. S. Weller and M. A. Biondi, Bull. Am. Phys. Soc. 13, 199 (1968); and Phys. Rev. 172, 198 (1968).